Coulomb blockade and hopping transport behaviors of donor-induced quantum dots in junctionless transistors[*]

Liu-Hong Ma(马刘红)[1,3], Wei-Hua Han(韩伟华)[2,3,†], and Fu-Hua Yang(杨富华)[3,4,‡]

[1] *School of Physics and Microelectronics, Zhengzhou University, Zhengzhou 450001, China*

[2] *Center of Materials Science and Optoelectronics Engineering, University of Chinese Academy of Sciences, Beijing 100049, China*

[3] *Engineering Research Center for Semiconductor Integrated Technology, Beijing Engineering Center of Semiconductor Micro-Nano Integrated Technology, Institute of Semiconductors, Chinese Academy of Sciences, Beijing 100083, China*

[4] *State Key Laboratory for Superlattices and Microstructures, Institute of Semiconductors, Chinese Academy of Sciences, Beijing 100083, China*

The ionized dopants, working as quantum dots in silicon nanowires, exhibit potential advantages for the development of atomic-scale transistors. We investigate single electron tunneling through a phosphorus dopant induced quantum dots array in heavily n-doped junctionless nanowire transistors. Several subpeaks splittings in current oscillations are clearly observed due to the coupling of the quantum dots at the temperature of 6 K. The transport behaviors change from resonance tunneling to hoping conduction with increased temperature. The charging energy of the phosphorus donors is approximately 12.8 meV. This work helps clear the basic mechanism of electron transport through donor-induced quantum dots and electron transport properties in the heavily doped nanowire through dopant engineering.

1. Introduction

In recent years, several novel materials have been proposed to keep up with the pace of Moore's law, such as carbon nanotubes and group III–V compound semiconductors.[1–3] Considering the device cost and the compatibility with silicon planar technology, research on new ideas for transistors based on silicon will continue. Dopants have a vital role in the semiconductor technology as passive charge providers. The aggressive scaling of transistors in the semiconductor industry has led to devices where only a few dopants determine the device electrical characteristics. The discreteness of dopant distribution will strongly affect the device operation.[4,5] On the other hand, this discreteness brings attractive applications based on the interplay between the potential modulations induced by individual dopants.[6,7] Single-electron transport mediated by individual dopants in silicon nanowire transistors was observed in previous experiments.[8–11] Dopant-induced quantum dot (QD) is considered as a promising candidate for the next generation of nano-electrical device, becoming the focus of quantum information. In this regard, systems of one-dimensional (1D) coupled QDs have attract much attention both in order to understand the underlying physics and to develop dopant-atom-based quantum transistors.

In the junctionless nanowire transistor (JNT), the doping concentration in the channel is identical to that in the source and drain.[12] Having no junction presents a great ad-

vantage, and accelerates the miniaturization of integrated circuits. When the gate voltage is lower than the flatband voltage, the carriers flow through a very narrow bulk conductive path in the center of the nanowire instead of a surface channel. The conductive path is gradually broadened until it forms a cross-section with increased gate voltage.[13] In the initial stage of subthreshold regime, an ultranarrow conduction path containing a few ionized donors is located near the center of the nanowire. In this case, a QD array is spontaneously formed and the carrier transports in the channel center.[14,15] As a novel approach for realizing multiple QDs, JNTs offer a variety of appealing physical properties. This design allows multiple coupled QDs to be arbitrarily positioned along a heavily-doped channel. Consequently, JNT can be used as a model system to study quantum transport effects in low dimensional systems. In particular, full control electron tunneling through donor-induced QDs should allow improvements in the study of spin and charge dynamics in nanowire.

In this paper, we report the formation of multiple coupled QDs that are fully defined by ionized donors in a long channel JNT. We discuss random dopant effects in the long channel junctionless transistor associated with quantum confinement effects. By collecting the transport spectra of multiple donor atoms in the channel of silicon FinFET, we present experimental evidence for the emergence of a coupled QDs system. Importantly, by analyzing the relationship between the activation

[†]Corresponding author. E-mail: weihua@semi.ac.cn

[‡]Corresponding author. E-mail: fhyang@semi.ac.cn

energy, charging energy, interaction energy of QDs and the thermal energy, we can obtain the impurity states and properties of electron transport through QDs. These researches are proofs to the importance of donor-induced QDs in ultrasmall silicon devices, highlight the earnestly requirement for a further understanding of the quantum transport mechanisms of multiple coupled ionized dopant atoms.

2. Device fabrication

The JNTs used in this study have the polysilicon gate wrapped around three sides of the silicon channel, scanning electron microscope (SEM) image and schematic diagram of the device structure are shown in Figs. 1(a) and 1(b), respectively. The devices consist of a heavily n-doped silicon nanowire connected to large source/drain electrodes. The channel of JNT has the same doping type and concentration as the drain and the source, with the phosphorus doping concentration of 1×10^{19} cm^{-3}. It is followed by a sacrificial oxidation to eliminate the etching induced damage as well as reduce the surface roughness. The final cross section of the silicon core is estimated to be 35 nm in height (H) and 30 nm in width (W), as shown in Fig. 1(c). A heavily doped polysilicon nanowire with the thickness of 300 nm, deposited perpendicular to the channel center and separated from it by a 22 nm thin silicon oxide, acts as a gate. Al electrodes are contacted with Ni/Si contact. The conventional operation of JNT is to apply a positive gate voltage to create an electroneutral region in the channel and allow electron to flow.
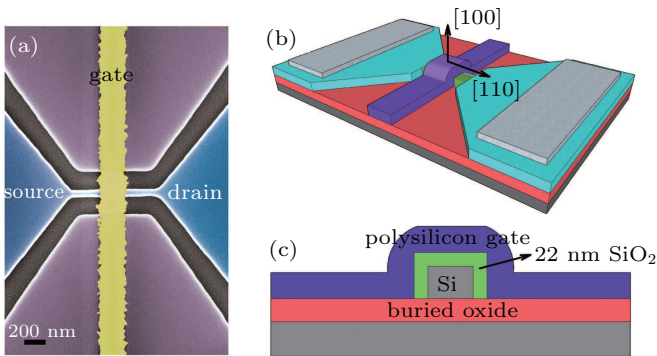

Fig. 1. (a) False color SEM image of device after the gate formation. The gate length is 280 nm and the channel has a cross section of 30 nm×35 nm. (b) A schematic diagram of the device structure, silicon nanowires are defined along the $\langle 110 \rangle$ direction. (c) Cross section schematics of the device, the SiO$_2$ dielectric layer is 22 nm.

3. Results and discussion

The fabricated device was measured at the temperature ranging from 6 K to 300 K. Figure 2(a) shows the transfer characteristics at room temperature. Without applied gate voltage, the channel electrons are fully depleted as a result of enough thin and narrow n-type silicon nanowire wrapped by the heavily p-type doped polysilicon gate. The drain leakage

current of less than 10 pA is obtained. The transfer characteristics manifest a subthreshold swing (SS) of 200 mV/dec, and the on/off current ratio of larger than 1×10^5 for $V_{DS} = 1.1$ V. The low field electron mobility μ_0 can be deduced from the Y-function method, which eliminates the influence of mobility degradation factor and series resistance, as given by[16,17]

$$Y = I_{DS}/\sqrt{g_m} = [(W_{eff}/L)C_{ox}\mu_0 V_{DS}]^{1/2} (V_{GS} - V_{TH}),$$

where C_{ox}, the gate capacitance per unit area, is estimated to be 1.56×10^{-7} F·cm^{-2} (≈ 22 nm gate oxide), L is the gate length, and the effective gate width W_{eff} is defined as $2H + W$. Figure 2(b) shows the transconductance (g_m) characteristic, the inset shows the Y-function plot. It is worth emphasizing that there are two kinds of slopes, S_1 and S_2, in the plot. In particular, the majority carriers can flow through the neutral conduction path without the influence of surface effects and perpendicular fields under the flatband condition. While above V_{FB}, a large number of electrons gather at the surface accumulation layer, the carrier mobility is seriously degenerated with increasing V_{GS} under the influence of surface effects and perpendicular fields. Therefore, these two kinds of slopes in Fig. 2(b) on the Y-function just manifest two different kinds of conduction mechanisms separated by V_{FB}, which can be extracted from the slope turning point of the Y-function.[18] Besides, the intercept of the S_1 line on the V_{GS} axis gives the threshold voltage V_{TH}.[17] Room temperature V_{TH} and V_{FB} are 0.47 V and 0.84 V, respectively. It is noted that V_{TH} is located far away from V_{FB} in JNT in comparison with that in the inversion-mode transistor. Figure 2(c) gives the temperature dependence of V_{TH} and V_{FB}. The low temperature Y-function shows multiple oscillations due to the quantum effect. Thus, V_{TH} and V_{FB} are only extracted for 75 K to 300 K, with the shift slopes up to 2.4 mV/K and 2.9 mV/K, respectively.

A possible error in the Y-function extraction of the low field mobility in the accumulation layer (extracted from the slope S_2) arises from the additional neutral current. However, the extracted low field mobility is well reliable because the error is very small.[19] The interface scattering can be neglected in JNT due to rather small perpendicular fields. μ_0 tends to increase with increasing temperature, resulting from decreased impurity scattering in the heavily doped JNT. At the temperatures higher than 200 K, the electron mobility is almost temperature independent (approximately 54 cm$^2 \cdot$V$^{-1} \cdot$s^{-1}), as the influences of temperature variation on impurity scattering and phonon scattering are almost compensatory.

In the ultra-thin channel, the electron is strongly confined in the nanowire center below the flatband region with the effect of depletion potential.[20] Consequently, the distribution of discrete donors induced QDs in the channel is more significant. In the JNT device, the quantum transport information

is easier to observe experimentally, which arises from the suppressed surface effects and perpendicular fields in comparison with those in the inversion-mode transistor. In order to study the effect of discrete donors induced QDs inside the nanowire, we need to investigate their electrical behaviors at low temperatures. The drain current characterizations tuned by the gate voltage were carefully measured in the temperatures ranging from 6 K to 80 K.
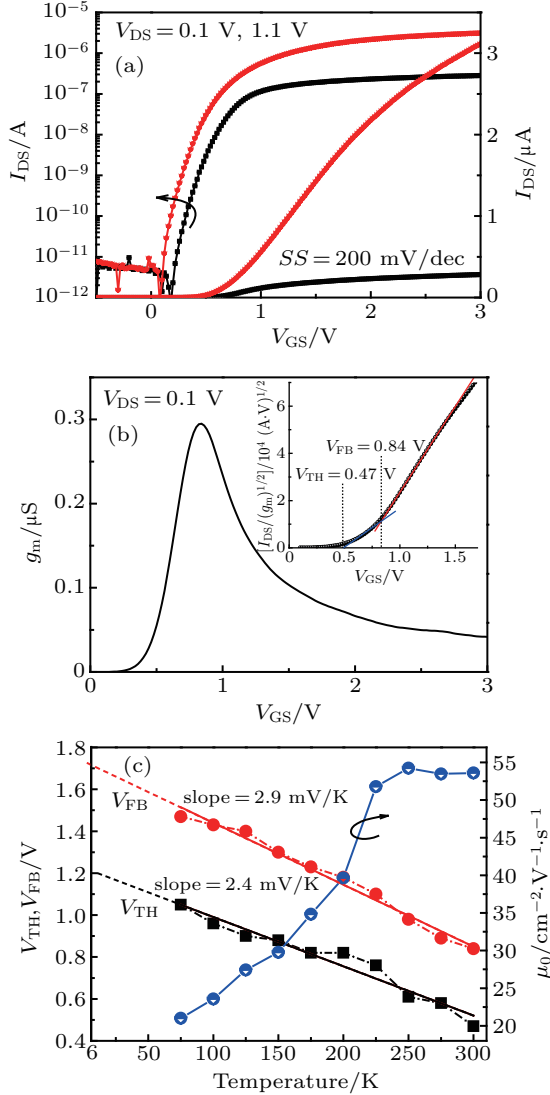

Fig. 2. (a) Drain current I_{DS} in JNT as a function of the gate voltage V_{GS} at room temperature. (b) The transconductance g_m as a function of V_{GS}. The inset shows the corresponding $I_{DS}/(g_m)^{1/2}$ plot. (c) Temperature dependence of V_{TH}, V_{FB}, and μ_0.

The current–voltage characteristics in dependence of the gate voltage at 6 K are shown in Fig. 3(a). The Coulomb blockade induces the appearance of a strongly suppressed conductance region at small V_{GS}, called Coulomb gap. The most striking effect is the variation in width of the zero conductivity region, which depends reversibly on large scale changes of V_{GS}. Negative gate voltages readily decrease the zero-conductance region, which almost disappears at high gate voltage of 2.5 V. This means that the tunnel capacitances and resistances are gate voltage dependent. The inset of Fig. 3(b)

manifests a comparative structure fabricated on the same wafer only without nanowire channel. The current–voltage characteristics of the heavily-doped Si film with Ni/Si contact are shown in Fig. 3(b). The structure exhibits linear I–V characteristics, suggesting good ohmic conductor. Hence, we ascribe the Coulomb gap to single electron transport mediated by a quantum system formed in the nanowire channel.
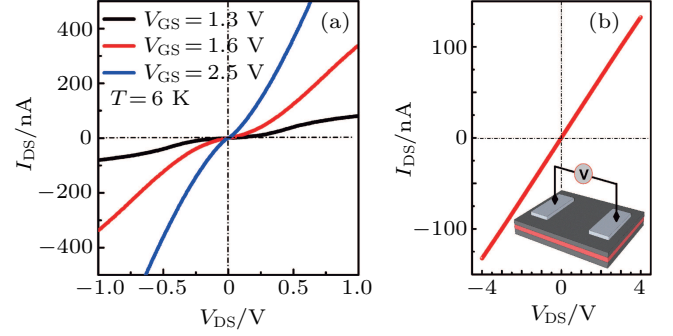

Fig. 3. (a) Coulomb blockade I_{DS}–V_{DS} characteristics of JNT at 6 K for different V_{GS}. (b) The current–voltage characteristics of the heavily-doped Si film with Ni/Si contact measured at 6 K. All specimens exhibit near linear I–V characteristics, suggesting good ohmic conductor.

The I–V curves for the JNT were measured at 6 K for various source–drain voltages V_{DS}. Figure 4(a) shows I_{DS} verses V_{GS} with V_{DS} ranging from 2 mV to 10 mV at 6 K. The low temperature V_{FB} is determined to be 1.72 V, according to the V_{GS} axis intercept of the temperature dependence of V_{FB}. Distinct two envelopes like current oscillations are observed below V_{FB}. At least five subpeaks can be distinguish from the transconductance characteristics within an envelope, as shown in Fig. 4(b), suggesting that single electron tunneling transport is modulated by a complex coupled QDs system.[21] There are no designed barriers in the channel. Therefore, the QDs formation has to be the result of natural quantum mechanism, most likely the random distribution of the ionized donors. We evaluate the dimensions of the QD from the V_{GS} period between consecutive envelops. The characteristics can be interpreted as the transport through five donors directly coupling to the delocalized states of the channel. The first Coulomb blockade envelope refers to the D^0 states and the second refers to the D^- states. The positions of the subpeaks are marked by black arrows in Fig. 4(b). Along the gate voltage axis, the average period of the D^0 state and D^- state is $\Delta V_g \approx 206$ mV, which corresponds to a gate capacitance of $C_g = e/\Delta V_g \approx 0.78$ aF. For an isolated spherical QD with radius r imbedded in the Si channel, the capacitance $C_g = 4\pi\varepsilon_0\varepsilon_r r$. The QD radius is estimated to be approximately 1.8 nm, agrees well with the Bohr radius for phosphorus atoms in silicon (the Bohr radius for phosphorus in silicon is about 2 nm). Consequently, the single-electron current oscillation is indeed arisen from the dopant induced QDs.

Below the flatband voltage, it is expected that a lowest potential path forms along the center axis of the channel due to

the action of the depletion potential around the nanowire, only a small number of donors in the central region of the slit will dominantly contribute to the formation of 1D QDs, which is illustrated in the insert of Fig. 5. In this case, an ionized donor introduces a Coulombic potential well that acts as an artificial QD, with a ground discrete state D^0 (the neutral state) and an excited state D^- (the negatively charged state). At the initial stage of transport, when the source Fermi level is aligned with the quantum states, it becomes easier to identify the envelope with several current subpeaks via coupling donors.[22,23]
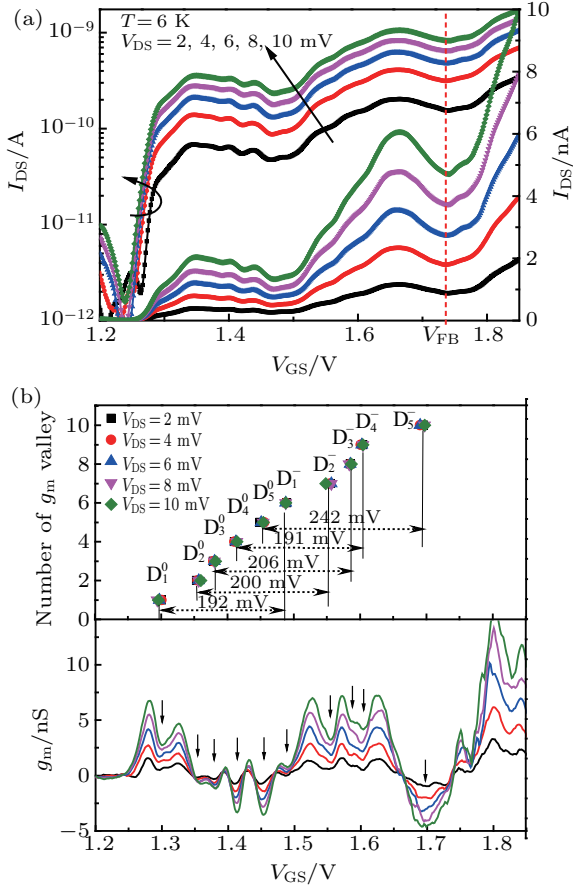

Fig. 4. (a) Drain current I_{DS} verses gate voltage V_{GS} and (b) the corresponding transconductance characteristics for different drain–source bias voltage V_{DS} ranging from 2 mV to 10 mV at 6 K. The Coulomb peaks appear in groups.
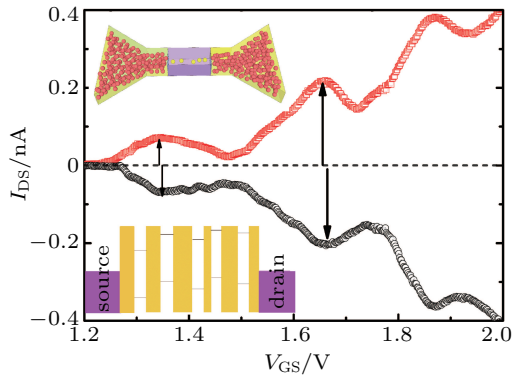

Fig. 5. The I_{DS}–V_{GS} curves for $V_{DS} = \pm10$ mV. The insert shows a representation of multiple phosphorous donors distributed along the channel below the flatband region and the formation of misaligned quantum levels.

The transfer curves for $V_{DS} = \pm10$ mV are plotted in Fig. 5. The single electron tunneling currents in both cases are almost comparable, i.e., the maximum tunneling currents are both approximately 1.1 nA. This observation manifests that the electron tunneling rates are not significantly affected by changing the polarity of V_{DS}. In contrast, the subpeak positions for the two cases are obviously different. This indicates that the distributions of donor-induced QDs are asymmetrical for the source and the drain, as illustrated in the insert of Fig. 5. This is fully consistent with the features of random doping. The quantum states of the donor dot are misaligned due to the random distribution of the randomly doped atoms, resulting in such low tunneling current at low temperature in the photon-assisted tunneling process.[24] The electron transport is extremely complicated in comparison with that in ordered QDs. To clarify the transport mechanisms in the disordered multiple-dot system, we turn to the thermal activation of the electron transport explored by the temperature dependence transfer characteristics. The current characteristics of the transistor versus V_{GS} were measured at several low temperatures up to 200 K by applying $V_{DS} = 10$ mV. The subthreshold conductance shows series of conductance peaks due to electron tunneling through a potential well in the conduction band, as shown in Fig. 6(a). The current envelopes remain visible up to 80 K. The inset of Fig. 6(a) provides the Arrhenius plots of conductance for D_1^0 position. Interestingly, three distinct regions are clearly observed, similar to those in the disordered QDs system.[25] At the temperatures lower than 30 K, resonant tunneling becomes the dominating conduction mechanism. Hence, the thermionic activated current is almost temperature independent. The observed Arrhenius-like T dependence at intermediate T (30 K $< T <$ 100 K) is a typical thermally activated process. From the slope of the Arrhenius plot, we obtain the activation energy (E_a) of 6.6 meV. We calculate the activation energies in this temperature range for the first five subpeaks, the activation energy falls between 5 meV and 7 meV. This activation energy corresponds to the energy difference activated hopping transport. In this region, the electron localized in a neutral (D^0) donor atom is able to be excited with the phonon-assistant energy to another un-occupied ground state of neighbor donor atom, the conductance varies as $G \propto \exp(E_a/k_BT)$. For the electron transport via coupled QDs, the activation energy is equivalent to the interaction energy of the QDs, which corresponds to the subpeak spacing energy. At the higher temperature ($T >$ 100 K), the thermal electron gains enough energy to escape from the localized state to the conduction band. Hence, the activation energy 23.6 meV corresponds to the level spacing between the silicon conduction band and the ground state of the QD, that is the blinding energy of electron in ground state for the donor-induced QD.
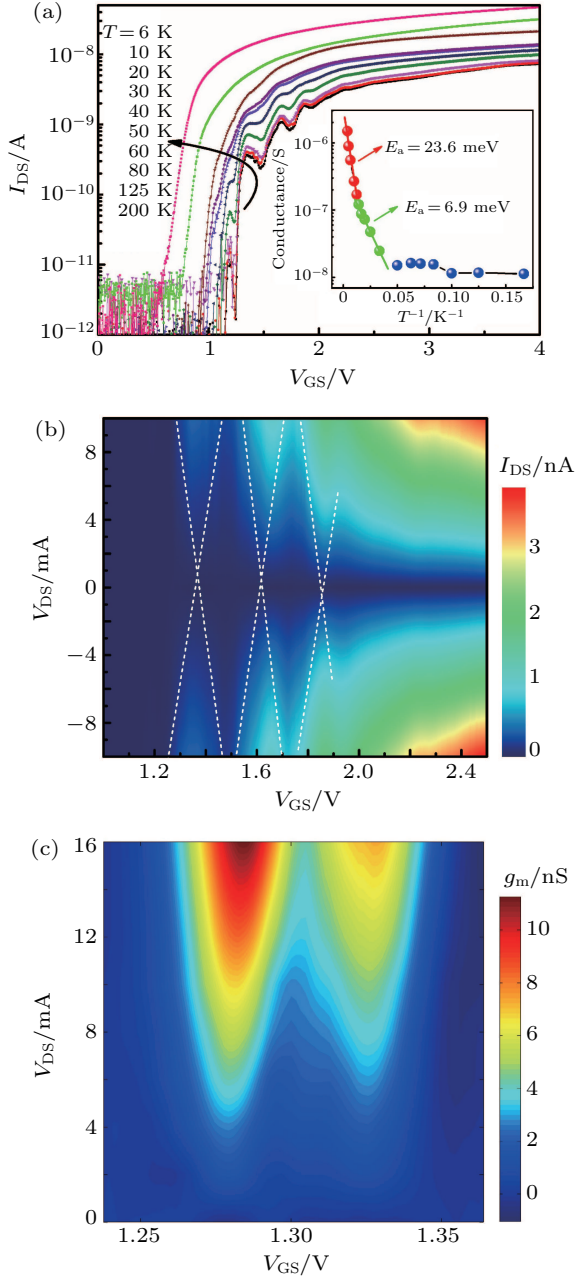
Fig. 6. (a) Temperature effect on the gate voltage-dependent conductance. The source–drain voltage is 10 mV. The insert shows Arrhenius plots of the conductance in different temperature regions for D_1^0 position. (b) The stability diagram of drain current at 6 K. (c) The contour diagram of the transconductance measured at 6 K.

Single electron charging energy is an essential parameter for determining the transport behaviors of QDs, representing the energy that an addition electron in the source Fermi sea moves into the QD. Figure 6(b) shows the stability diagram of current in color scale where clear Coulomb blockade diamonds are visible. The positive slope is given by $C_g/(C_d+C_g)$ and the negative slope equals C_g/C_s, where C_d and C_s are the coupling capacitances between the donor and the source and drain, respectively. Then we obtain $C_s = 7.2C_g$, $C_d = 7.9C_g$, and the total capacitance $C_\Sigma = C_g + C_d + C_s = 12.5$ aF. The diagram exhibits the Coulomb diamond of the charging energy on the order of 12.8 meV, lower than the activation energy in the

high temperature region, in good agreement with the charging energy of 12.6 meV extracted from the contour diagram of transconductance presented in Fig. 6(c). The Coulomb blockade should not be affected unless the thermal energy exceeds half of the charging energy. Hence, the current oscillations should remain visible up to a temperature of 74 K, agree well with the temperature dependent current shown in Fig. 6(a). Then the lever arm factor $\alpha = C_g/C_\Sigma$ equals 0.065, the small conversion factor could be attributed to the relatively thick gate oxide and depletion layer. In the model proposed by Altermatt *et al.*, the blinding energy of the ground state electron for Si : P is 2.1 meV depending on the doping concentration of 1×10^{19} cm^{-3} in bulk Si material.[26] As expected, the charging energy and activation energy in the high temperature region should extremely small for phosphorus in silicon. Nevertheless, the energies obtained in this experiment differ sharply from the Altermatt model due to the spatial localization. Previous studies have shown that the blinding energy of the dopants is largely enhanced by the confined environment.[27–29] In JNT, the initial conduction path is ultra-narrow, forming enhanced blinding effect. As a consequence, the dopant blinding energy and the charging energy are both enhanced through quantum confinement and dielectric confinement.

4. Conclusion

In summary, we fabricated junctionless transistors with multiple QDs formed by a few closely-spaced phosphorus donors. Low temperature I_{DS}–V_{GS} measurements can offer transport spectroscopy information about resonant tunneling within 1D QDs conduction path containing a few donor atoms. The temperature-dependent activation energies have profound implications for the electron transport behaviors, changing from cotunneling transport to hopping transport with increased temperature. We have identified the D^0 neutral states and D^- charge states for individual phosphorus donors, the charging energy is measured to be 12.8 meV. Besides, the enhancement effect of the confinement environment for the donor blinding energy has been investigated. Our experiments suggest that single electron tunneling can be medicated by multiple dopants in the channel center even in the dopant rich environment. The experiments provide understanding of the atomic properties of coupled dopant atoms. As such, these results are highly relevant to the development of Si : P nanoelectronics.

References

[1] Cao Q, Tersoff J, Farmer D B, Zhu Y and Han S J 2017 *Science* **356** 1369

[2] Sun S X, Ma L H, Cheng C, Zhang C, Zhong Y H, Li Y X, Ding P and Jin Z 2017 *Phys. Status Solidi A* **214** 1700322

[3] Sun S X, Chang M M, Li M K, Ma L H, Zhong Y H, Li Y X, Ding P, Jin Z and Wei Z C 2019 *Chin. Phys. B* **28** 078501

[4] Li Y, Yu S M, Hwang J R and Yang F L 2008 *IEEE Trans. Electron Devices* **55** 1449

[5] Shine G and Saraswat K C 2017 *IEEE Trans. Electron Devices* **64** 3768

[6] Akhavan N D, Ferain I, Yu R, Razavi P and Colinge J P 2012 *Solid State Electron.* **70** 92

[7] Moraru D, Samanta A, Tyszka K, Muruganathan M, Mizuno T, Jablonski R, Mizuta H and Tabe M 2015 *Nanoscale Res. Lett.* **10** 372

[8] Fuechsle M, Miwa J A, Mahapatra S, Ryu H, Lee S, Warschkow O, Hollenberg L C L, Klimeck G and Simmons M Y 2012 *Nat. Nanotechnol.* **7** 242

[9] Pierre M, Wacquez R, Jehl X, Sanquer M, Vinet M and Cueto O 2009 *Nat. Nanotechnol.* **5** 133

[10] Tabe M, Moraru D, Ligowski M, Anwar M, Jablonski R, Ono Y and Mizuno T 2010 *Phys. Rev. Lett.* **105** 016803

[11] Uddin W, Georgiev Y M, Maity S and Das S 2017 *J. Phys. D: Appl. Phys.* **50** 365104

[12] Colinge J P, Lee C W, Afzalian A, Akhavan N D, Yan R, Ferain I, Razavi P, O'Neill B, Blake A, White M, Kelleher A M, McCarthy B and Murphy R 2010 *Nat. Nanotechnol.* **5** 225

[13] Colinge J P, Lee C W, Afzalian A, Akhavan N D, Yan R, Ferain I, Razavi P, O'Neill B, Blake A, White M, Kelleher A M, McCarthy B and Murphy R 2010 *Nat. Nanotechnol.* **5** 225

[14] Moraru D, Ligowski M, Yokoi K, Mizuno T and Tabe M 2013 *Appl. Phys. Express* **2** 071201

[15] Ma L H, Han W H, Zhao X S, Guo Y Y, Dou Y M and Yang F H 2018 *Chin. Phys. B* **27** 088106

[16] Lee C W, Borne A, Ferain I, Afzalian A, Yan R, Akhavan N D, Razavi P and Colinge J P 2010 *IEEE Trans. Electron Devices* **57** 620

[17] Ghibaudo G 1988 *Electron. Lett.* **24** 543

[18] Ma L H, Han W H, Wang H, Yang X and Yang F H 2015 *Chin. Phys. B* **24** 128101

[19] Jeon D Y, Park S, Mouis M, Berthome M, Barraud S, Kim G T and Ghibaudo G 2013 *Solid-State Electron.* **90** 86

[20] Duarte J P, Kim M S, Choi S J and Choi Y K 2012 *IEEE Trans. Electron Devices* **59** 1008

[21] Waugh F R, Berry M J, Mar D J, Westervelt R M, Campman K L and Gossard A C 1995 *Phys. Rev. Lett.* **75** 705

[22] Tan K Y, Chan K W, M, Morello A, Yang C, Donkelaar J V, Alves A, Pirkkalainen J M, Jamieson D N, Clark R G and Dzurak A S 2010 *Nano Lett.* **10** 11

[23] Sellier H, Lansbergen G P, Caro J, Rogge S, Collaert N, Ferain I, Jurczak M and Biesemans S 2006 *Phys. Rev. Lett.* **97** 206805

[24] Morgan N Y, Abusch-Magder D, Kastner M A, Takahashi Y, Tamura H and Murase K 2001 *J. Appl. Phys.* **89** 410

[25] Romero H E and Drndic M 2005 *Phys. Rev. Lett.* **95** 156801

[26] Altermatt P, Schenk A and Heiser G 2006 *J. Appl. Phys.* **100** 113714

[27] Wang H, Han W H, Ma L H, Li X M, Hong W T and Yang F H 2014 *Appl. Phys. Lett.* **104** 133509

[28] Diarra M, Niquet Y M, Delerue C and Allan G 2007 *Phys. Rev. B* **75** 045301

[29] Björk M T, Schmid H, Knoch J, Riel H and Riess W 2009 *Nat. Nanotechnol.* **4** 103